Human Molecular Genetics, 2016, Vol. 25, No. 4 706–714

doi: 10.1093/hmg/ddv508
Advance Access Publication Date: 17 December 2015
Original Article

ORIGINAL ARTICLE

Tissue-specific modulation of mitochondrial DNA segregation by a defect in mitochondrial division

Riikka Jokinen[1], Paula Marttinen[1], James B. Stewart[2], T. Neil Dear[3] and Brendan J. Battersby[1,*]

[1]Research Programs Unit – Molecular Neurology, University of Helsinki, Helsinki, Finland, [2]Max Planck Institute for Biology of Ageing, Cologne, Germany and [3]South Australian Health and Medical Research Institute, Adelaide, Australia

*To whom correspondence should be addressed at: Research Programs Unit, University of Helsinki, Haartmaninkatu 8 r.C524b, 00290 Helsinki, Finland. Tel: +358 504486390; Fax: +358 919125610; Email: brendan.battersby@helsinki.fi

Abstract

Mitochondria are dynamic organelles that divide and fuse by remodeling an outer and inner membrane in response to developmental, physiological and stress stimuli. These events are coordinated by conserved dynamin-related GTPases. The dynamics of mitochondrial morphology require coordination with mitochondrial DNA (mtDNA) to ensure faithful genome transmission, however, this process remains poorly understood. Mitochondrial division is linked to the segregation of mtDNA but how it affects cases of mtDNA heteroplasmy, where two or more mtDNA variants/mutations co-exist in a cell, is unknown. Segregation of heteroplasmic human pathogenic mtDNA mutations is a critical factor in the onset and severity of human mitochondrial diseases. Here, we investigated the coupling of mitochondrial morphology to the transmission and segregation of mtDNA in mammals by taking advantage of two genetically modified mouse models: one with a dominant-negative mutation in the dynamin-related protein 1 (Drp1 or Dnm1l) that impairs mitochondrial fission and the other, heteroplasmic mice segregating two neutral mtDNA haplotypes (BALB and NZB). We show a tissue-specific response to mtDNA segregation from a defect in mitochondrial fission. Only mtDNA segregation in the hematopoietic compartment is modulated from impaired Dnm1l function. In contrast, no effect was observed in other tissues arising from the three germ layers during development and in mtDNA transmission through the female germline. Our data suggest a robust organization of a heteroplasmic mtDNA segregating unit across mammalian cell types that can overcome impaired mitochondrial division to ensure faithful transmission of the mitochondrial genome.

Introduction

Mammalian mitochondrial DNA (mtDNA) is transmitted through the female germline undergoing both purifying selection and a genetic bottleneck leading to the rapid segregation of mtDNA variants or mutations between generations (1–6). The exact timing of the genetic bottleneck is still debated (7) and proposed to occur either embryonically during expansion of the primordial germ cells or in post-natal folliculogenesis (4,5). Nonetheless, there is consensus that a small number of segregating units account for the rapid segregation of mtDNA variants from mother to offspring.

The mitochondrial genome is compacted by Tfam into a discreet structure called a nucleoid that is on average 70 nm in diameter in mammals, can contain one or more genomes, and also cluster heterogeneously within a mitochondrial network (8–10). Although other proteins are found within nucleoids (11,12) the predominant factor and structural organizer is Tfam (8). How nucleoids are organized as a segregating unit remains poorly understood, but is critical to the genetics of mtDNA.

Received: September 21, 2015. **Revised and Accepted:** December 8, 2015

In mammals no active mechanism has been described to date ensuring equal distribution of mtDNA molecules to daughter cells at cytokinesis (13), but the regulation of mitochondrial morphology is critical for maintenance of the mitochondrial genome. Disruptions to the mitochondrial fusion, but not fission, machinery are associated with mtDNA depletion and integrity (14,15). Moreover, mitochondrial nucleoids are found at the tips of recently divided mitochondria, a feature conserved from yeast to mammals (16–18).

Mitochondrial membrane dynamics are coordinated by dynamin-related GTPases that induce curvature in the mitochondrial outer and inner membrane for fusion or fission of the organelle (15). Dnm1l (Drp1) is the master regulator of mitochondrial fission. The protein is recruited as a dimer from the cytosol to the surface of the outer membrane assembling by self-oligomerization as a constricting ring around the organelle with GTP hydrolysis providing the power stroke to induce membrane deformation and fission (19–21). Defects in Dnm1l function, by genetic silencing or dominant-negative mutations, impair fission leading to hyperfusion of the mitochondrial network. However, the complete loss of Dnm1l function leads to collapse of the mitochondrial network around the nucleus (22,23), and embryonic lethality (24,25). Also, conditional deletion of *Dnm1l* in the female germline impairs oocyte maturation and thereby compromises fertility (26). So far, only mutations in the middle domain of Dnm1l, important for multimer assembly, are compatible with mammalian development but these mutations are still pathogenic post-natally in a tissue-specific manner (27,28). Thus, the penetrance of Dnm1l inhibition on mitochondrial fission determines the severity to cellular fitness and embryonic development.

During preimplantation embryogenesis there is strict regulation on mtDNA copy number and mitochondrial gene expression, and dynamic remodeling of mitochondrial morphology. Replication of the ~200 000 copies of mtDNA in the mouse embryo (4,5) is repressed following fertilization of the mature oocyte and the initiation of blastomere cleavage. Only following successful implantation of the blastocyst to the uterine wall reactivates mtDNA replication (29). A minimum mtDNA copy number of ~40 000 in mouse oocytes is required for successful implantation (30). Nonetheless, mitochondrial gene expression is active during the preimplantation embryogenesis period with transcription and ribosome biogenesis occurring (31) in tandem with dramatic changes to mitochondrial morphology and ultrastructure. All of the mitochondrial dynamin-related GTPases that coordinate fission and fusion are expressed during embryogenesis (32) and, yet, in mature human and mouse oocytes mitochondria are spherical, separate organelles with few cristae, whereas by the blastocyst stage the organelle obtains a more elongated morphology with a developed cristae ultrastructure (33,34).

Reduction of Dnm1l abundance in an aneuploid cancer cell line heteroplasmic for the A3243G mitochondrial mutation in the $tRNA^{Leu(UUR)}$ led to an accumulation of the mutation in clones (35). However, the segregation of mtDNA variants and pathogenic mutations in cultured cells is highly variable and fails to replicate the patterns seen *in vivo* in human and mouse tissues (36). This demonstrates the importance of studying the complexity of mtDNA genetics and, in particular, the segregation of heteroplasmic variants in animal models.

To circumvent these difficulties we used two different mouse models to investigate the coupling of mitochondrial morphology to the transmission and segregation of mtDNA. The Python mouse model is heterozygous for a C452F mutation in the middle domain of Dnm1l ($Dnm1l^{Py}$) that impairs multimer assembly and therefore mitochondrial fission generating a hyperfused mitochondrial network (Fig. 1) (28). This Dnm1l mutation can be stably transmitted through both the male and female germline with normal Mendelian ratios, but is embryonic lethal when homozygous (28). Python mice only develop a dilated cardiomyopathy that leads to congestive heart failure in older animals even though the C452F mutation is present in all Dnm1l isoforms and expressed in all tissues (28). The other mouse model we use is heteroplasmic for two non-pathogenic mtDNA haplotypes called BALB and NZB (3), which do not appear to encode differences that affect the mitochondrial respiratory chain function (37,38) or mtDNA replication (37). The transmission of these variants through the female germline is by random genetic drift (3), a pattern also seen in the transmission of some pathogenic point mutations in both humans and mice (39–40). These heteroplasmic mice display a post-natal tissue-specific selection for mtDNA haplotypes only in the liver, kidney and hematopoietic tissues, processes regulated by different mechanisms and genes (37,41–45). In all other tissues the segregation of these mtDNA haplotypes is random (41).

Here, we show a tissue-specific modulation in mtDNA segregation from impaired mitochondrial fission. Only in the hematopoietic compartment did dysfunctional Dnm1 l affect mtDNA segregation. In contrast, there was no effect on mtDNA segregation in all other tissues examined. Moreover, there was no effect on the random genetic drift of mtDNA heteroplasmy in the offspring. This points to a robust organization of the mtDNA segregating unit across tissues and throughout development, but apparently different in leukocytes.

Results

No effect of impaired mitochondrial division on mtDNA transmission through the germline

We established continuous breeding of heteroplasmic Python ($Dnm1l^{+/Py}$) and wild-type females from 7 weeks of age generating up to 3 litters to avoid any complications from the onset of heart failure in Pythons. No difference was observed in the timing between litters and weaning, or in the expected Mendelian ratios of these alleles (Supplementary Material, Table S1). The number of pups from the first and subsequent litters of $Dnm1l^{+/Py}$ mothers was no different than wild-type, but a few females did have small litters consisting of only two pups (Fig. 2A).

To test whether the C452F mutation in Dnm1l affected the transmission of mtDNA heteroplasmy we compared the percentage of NZB mtDNA in the offspring to the level in the mother using a modified Kimura distribution, as it best represents mtDNA heteroplasmy with random genetic drift and no selection (46). In some cases, we pooled the offspring data from mothers with a similar heteroplasmy level to increase the statistical power of our analysis (7). We were unable to reject the null hypothesis as defined by a Kimura distribution, thus demonstrating a neutral germline transmission in both $Dnm1l^{+/+}$ and $Dnm1l^{+/Py}$ mothers (Fig. 2, Table 1). Our data suggest that a defect in mitochondrial fission with the C452F Dnm1l mutation has no effect on the segregating unit of mtDNA during transmission through the genetic bottleneck of the female germline.

The effect of impaired mitochondrial division on mtDNA segregation across tissues

Next, we assessed in 90-day-old mice the mtDNA heteroplasmy level across tissues arising from the three germ layers: brain

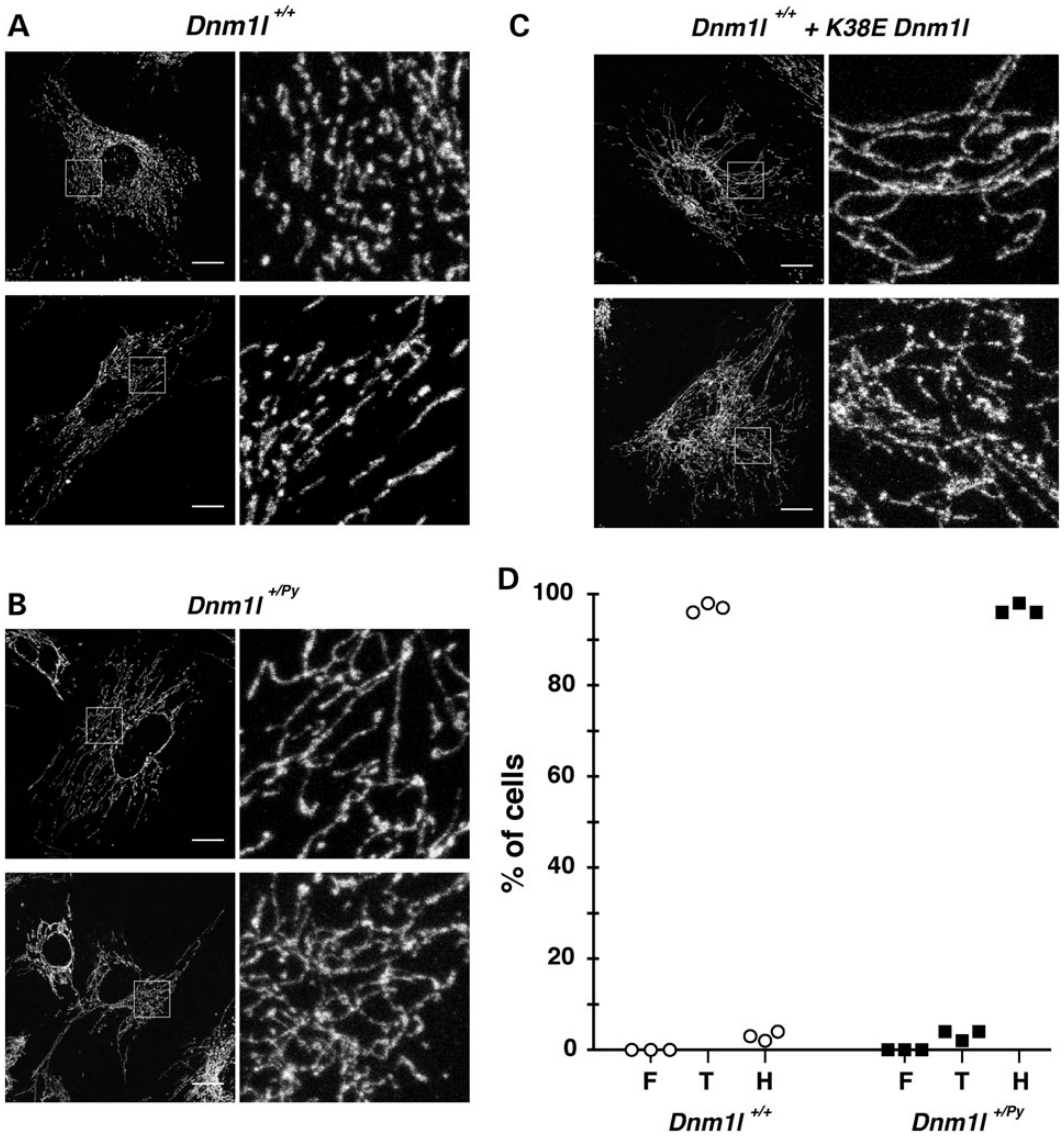

Figure 1. Impaired mitochondrial division with the C452F (Py) Dnm1l mutation. Representative maximal projection confocal images of antibody staining against the mitochondrial protein Sdha in MEFs isolated from (**A**) *Dnm1l*$^{+/+}$ and (**B**) *Dnm1l*$^{+/Py}$ mice. (**C**) The K38E Dnm1l cDNA was transfected into *Dnm1l*$^{+/+}$ MEFs as a positive control, as it is a well-known dominant-negative mutant, that disrupts mitochondrial fission and generates a hyperfused network. Two representative images are shown for each genotype. (**D**) Quantification of mitochondrial morphology in *Dnm1l*$^{+/+}$ and *Dnm1l*$^{+/Py}$ MEFs from three independent biological replicates ($n = 100$ cells for each replicate). Mitochondria were classified as fragmented (**F**), tubular (**T**) or hyperfused (**H**). The scale bar is 20 μm.

and skin (ectoderm); heart and skeletal muscle (mesoderm) and small intestine (endoderm). In these tissues, the percentage of NZB mtDNA is indistinguishable from each other at birth and with age (41,42); thus, these tissues do not display selection for either haplotype and are considered neutral with respect to mtDNA segregation. This concordance in mtDNA heteroplasmy levels across tissues is also seen for pathogenic mtDNA point mutations (40).

To test whether a defect in mitochondrial fission affects the segregation of mtDNA in these tissues we performed pairwise non-linear regression analysis of the mtDNA heteroplasmy level (Fig. 3). We used the mtDNA heteroplasmy level in the brain as a reference for each tissue comparison and constrained the line fit to go through the origin because it best models the situation biologically when animals are homoplasmic. Thus, deviations from a slope of 1 would indicate a difference in mtDNA segregation between tissues, where >1 indicates a preference for the NZB haplotype and <1 for the BALB mtDNA haplotype. Across these four tissues, the slope was close to 1 between tissues from wild-type and *Dnm1l*$^{+/Py}$ littermates. This is in contrast to the liver and spleen where there is skewed segregation of mtDNA haplotypes (Figs 4A and 5A).

mtDNA segregation in the liver

Previous work in these heteroplasmic mice has demonstrated that there is age-dependent selection for mtDNA haplotypes in the liver and spleen, which is regulated by different mechanisms and nuclear-encoded genes (37,41–44). In the liver there is selection of the NZB genome (37,41). The regression analysis for the NZB mtDNA level in the liver in a pairwise comparison with the brain demonstrates a positive slope deviating from 1 as expected for wild-type but also for *Dnm1l*$^{+/Py}$ littermates (Fig. 4A). To assess the mtDNA selection in the liver we calculated the relative

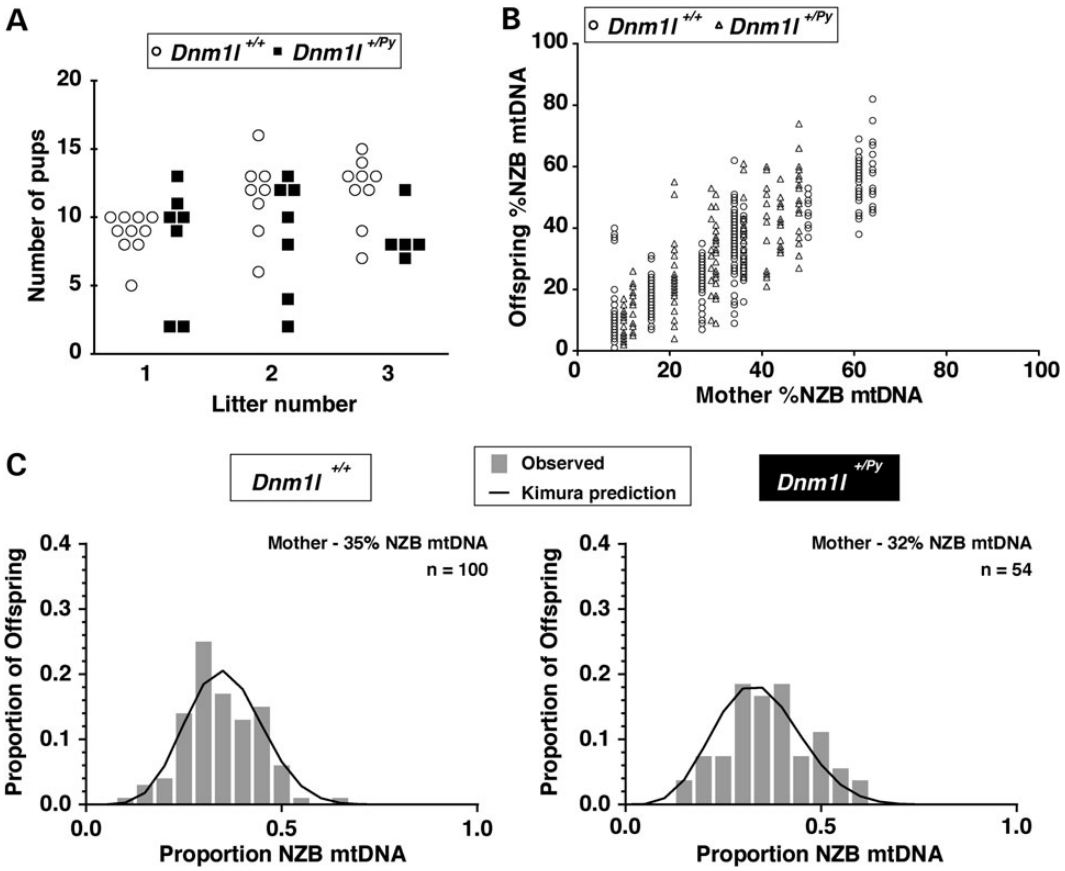

Figure 2. Random drift in the transmission of mtDNA through the female germline with the C452F (Py) Dnm1l mutation. (**A**) The number of progeny per litter generated from females with the indicated genotypes engaged in continuous breeding. (**B**) mtDNA heteroplasmy distribution in offspring from mothers with the indicated genotypes. (**C**) Representative data plots of the observed offspring distributions of the NZB mtDNA haplotype proportion compared with the expected neutral model [Kimura distribution (solid black line)]. No significance difference was detected in the offspring distributions.

Table 1. Tests of neutral transmission of the NZB mtDNA haplotype

Genotype	*p*	*var*	N	P-value	Females used
Dnm1l$^{+/+}$	0.16	0.00338	34	0.910	1069 WT
	0.35	0.00889	100	0.012	1105 WT, 1106 WT, 1113 WT
Dnm1l$^{+/Py}$	0.21	0.01273	28	0.178	1111 HZ
	0.31	0.01382	54	0.124	1101 HZ, 1104 HZ, 1112 HZ
	0.44	0.01514	46	0.052	1102 HZ, 1103 HZ, 1115 HZ

Females were grouped by their relative proportion of the NZB haplotype (*p*), and the variance in offspring NZB haplotype proportions (*var*) and the number of offspring (*N*) were calculated from the relative NZB levels from the offspring. Transmission was tested versus the neutral Kimura distribution for the transmission of mtDNA variants. The *P*-value for each test is reported, but to determine significance Sidak's adjustment was used to correct for multiple testing ($\alpha = 0.0073$).

fitness for the NZB mtDNA haplotype as a function of age (37). We found no difference between wild-type and Python mice (Fig. 4B) suggesting that defects in mitochondrial fission do not modulate the mechanism of selection for the NZB haplotype in this tissue.

Defects in mitochondrial fission alter mtDNA segregation in the spleen

In the hematopoietic compartment of these heteroplasmic mice, there is selection against the NZB haplotype so that the BALB haplotype accumulates. The mechanism is active in all hematopoietic tissues, all leukocyte populations independent of lineage and independent of adaptive immune surveillance within the mice (43). This mtDNA selection is best modeled as an exponential decay (43). So far, this model applies to leukocytes from both mice and humans (modeled with A3243G tRNA^{Leu} mutation) with the only difference the rate, which is ~70 times faster in mice than humans (43,47). As expected the pairwise comparison of the heteroplasmy level in the spleen against the brain shows a significant deviation in the slope <1 (Fig. 5A).

To test if there was a difference in the splenic mtDNA selection we calculated the proportion of the NZB mtDNA remaining in the tissue (43). Here, we found that disruptions to mitochondrial morphology in the spleen modulated mtDNA segregation. The proportion of NZB mtDNA in the spleen of *Dnm1l*$^{+/Py}$ mice was significantly less ($P = 0.0028$) compared to wild-type littermates

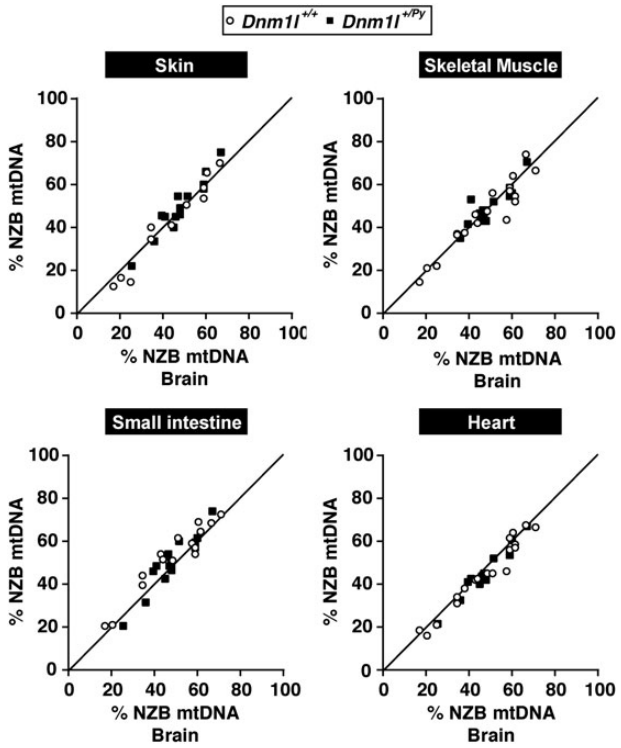

Figure 3. mtDNA segregation in the heart, skeletal muscle, skin and small intestine with the C452F (Py) Dnm1l mutation. Non-linear regression analysis of mtDNA levels in the indicated tissues compared with the brain in mice with the indicated Dnm1l genotypes. A line plot for a slope of 1.0 is indicated. Sample sizes and slopes in *Dnm1l*$^{+/+}$: heart ($n = 18$, 0.95); skeletal muscle ($n = 18$, 0.97); skin ($n = 11$, 0.97) and small intestine ($n = 16$, 1.07). Sample sizes and slopes in *Dnm1l*$^{+/Py}$: heart ($n = 15$, 0.95); skeletal muscle ($n = 14$, 1.00); skin ($n = 14$, 1.04) and small intestine ($n = 15$, 1.05).

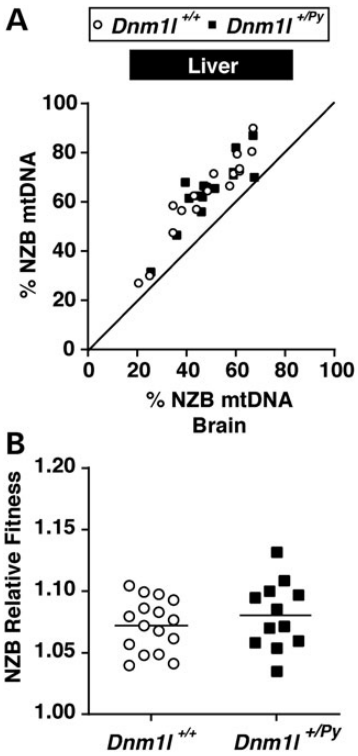

Figure 4. mtDNA segregation in the liver with the C452F (Py) Dnm1 l mutation. (**A**) Non-linear regression analysis of mtDNA levels in the liver compared with the brain in mice with the indicated Dnm1l genotypes. A line plot for a slope of 1.0 is indicated. Sample sizes and slopes in *Dnm1l*$^{+/+}$: liver ($n = 16$, 1.29). Sample sizes and slopes in *Dnm1l*$^{+/Py}$: liver ($n = 16$, 1.30). (**B**) Relative fitness for the NZB mtDNA haplotype in the liver as a function of age. The mean is indicated with the solid line. No significant difference between Dnm1 l genotypes.

(Fig. 5B). Thus, a disruption to mitochondrial fission appears to enhance the selection against the NZB haplotype.

Next, we tested whether the difference in mtDNA selection in the spleen was due to alterations in mtDNA copy number. We determined mtDNA copy number relative to a single-copy nuclear gene β-2-microglobulin by quantitative polymerase chain reaction (qPCR), and found no difference between the spleens of *Dnm1l*$^{+/+}$ and *Dnm1l*$^{+/Py}$ mice (Fig. 5C). Moreover, there was no concordance between mtDNA copy number and the proportion of NZB mtDNA in the spleen (Fig. 5C). These data indicate that the modulation of mtDNA segregation in the mouse spleen is not dependent upon alterations to mtDNA copy number.

There are no previous reports investigating the hematopoietic compartment in the Python mice, so we wanted to rule out whether a potential development defect in this tissue accounted for the effect on mtDNA heteroplasmy levels. Blood was taken by cardiac puncture from *Dnm1l*$^{+/Py}$ and wild-type littermates before the onset of congestive heart failure in the Python mice. We found no significant differences in the cellularity of the blood or other hematological parameters that would be suggestive of a developmental defect or abnormality in the Python mice (Supplementary Material, Fig. S1).

Discussion

In this study, we show a tissue-specific response to mtDNA segregation from a defect in mitochondrial fission. Only mtDNA segregation in the hematopoietic compartment is modulated by impaired Dnm1l function. In contrast, no effect was observed in other tissues or in transmission of the mitochondrial genome through the female germline.

The dynamics of mitochondrial membrane morphology play a key role in the inheritance and segregation of the mitochondrial genome (15). Fusion of the outer and inner membrane appears to be integral for maintaining mtDNA abundance and integrity (14). Deletion of both mitofusin 1 and mitofusin 2, the non-redundant dynamin-related GTPases that coordinate mitochondrial outer membrane fusion in mammals, in mouse skeletal muscle leads to mtDNA depletion and the accumulation of point mutations and deletions (14). In contrast, a disruption to mitochondrial division in the *Dnm1l*$^{+/Py}$ mice does not appear to adversely affect mtDNA copy number (28). Work from another group using a neonatal heart and skeletal muscle-specific Dnm1 l knockout found no difference in the cardiac mtDNA copy number at birth, but did find a post-natal defect in the coordination of mtDNA replication with heart growth, although these mice die by post-natal day 11 (22).

A model linking mitochondrial division with mtDNA segregation is beginning to emerge mainly from research in the budding yeast *Saccharomyces cerevisiae* with many features conserved in mammals (15). The first step in division is wrapping of the endoplasmic reticulum (ER) around mitochondria (48) marking the recruitment spot for Dnm1l dimers onto receptors resident on the mitochondrial surface. Oligomerization and activation of Dnm1l leads to constriction and ultimately fission of the membrane into two daughter mitochondria. ER wrapping of mitochondria is independent of Dnm1l and one of its receptors Mff (48). In yeast,

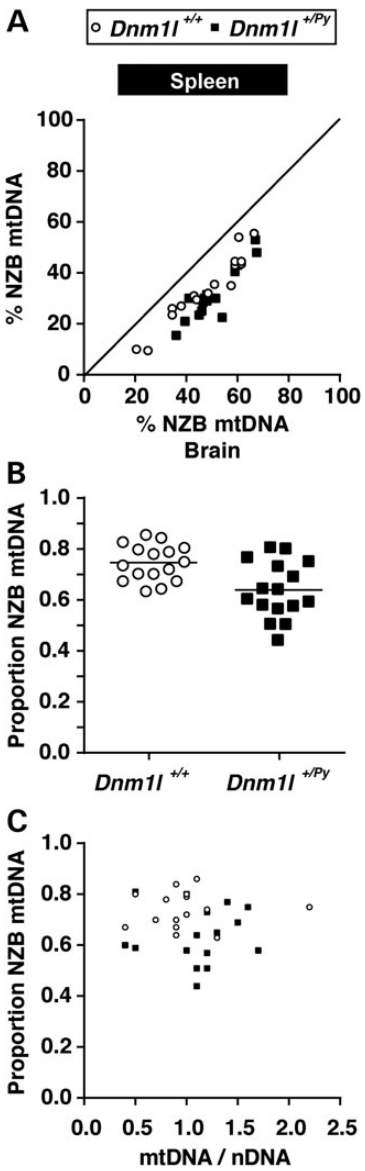

Figure 5. The C452F (Py) Dnm1l mutation modulates mtDNA segregation in the spleen. (**A**) Non-linear regression analysis of mtDNA levels in the spleen compared with the brain in mice with the indicated Dnm1l genotypes. A line plot for a slope of 1.0 is indicated. Sample sizes and slopes in *Dnm1l*$^{+/+}$: spleen ($n = 16$, 0.73). Sample sizes and slopes in *Dnm1l*$^{+/Py}$ spleen ($n = 15$, 0.63). (**B**) The proportion of NZB mtDNA in the spleen relative to a neutral tissue (skeletal muscle) in mice with the indicated genotypes, $n = 16$ in each group. Difference between *Dnm1l*$^{+/+}$ and *Dnm1l*$^{+/Py}$ mice was significantly different ($P = 0.0028$, two-tailed *t*-test). The solid black line indicates the mean. (C) mtDNA copy number relative to the proportion of NZB mtDNA in the spleen of mice with the indicated genotypes.

a molecular complex called ERMES (ER-mitochondrial encounter structure) is required to tether this inter-organellar contact (49) and also tightly associates with mtDNA nucleoids (18). Impaired assembly of the ERMES complex disrupts the nucleoid structure and causes mtDNA depletion (15). It is thought that this ER-associated mitochondrial division ensures equal segregation of mtDNA nucleoids to the tips of daughter mitochondria. In mammals the ERMES complex is not conserved but nucleoids are still found at the tips of dividing mitochondria (16,17), indicating the possibility of an analogous tethering structure in mammals.

The organization of the mitochondrial nucleoids as a segregating unit remains poorly understood. Advances in super resolution light microscopy have provided greater insight into the nucleoid mtDNA copy number and distribution within the organelle (9,10). How heteroplasmy is organized within an organelle at a cytological level of resolution is an important question that has not been addressed experimentally due to technical limitations in imaging two mtDNA haplotypes, let alone pathogenic single point mutations. Current methodologies provide only a static picture of nucleoid organization within the organelle and cannot address what constitutes a segregating unit, which is especially relevant for understanding in greater detail the genetics of mtDNA heteroplasmy and therefore most human pathogenic mtDNA mutations. Thus, the segregating unit could be a nucleoid composed of a single genome, multiples or clusters of nucleoids within close physical proximity. Future work is required to provide insight into these questions.

Our genetic approach in mice suggests a robust organization of a heteroplasmic segregating unit across mammalian cell types that appear to overcome impaired mitochondrial division to ensure faithful transmission of the mitochondrial genome. In the absence of selection, the segregation of mitochondrial genomes is best modeled as a random walk (50). Two factors are important for this process: mtDNA copy number and turnover. The best example of copy number is the genetic bottleneck in the female germline that leads to the rapid segregation of mtDNA variants. Our data demonstrate that impaired division has no effect on the segregation of mtDNA haplotypes through the female germline in mice. To establish a newborn mouse requires a minimum of 24 cell divisions (51), changes to cell size, mtDNA copy number and differentiation, and yet tissues derived from all three germ layers have indistinguishable mtDNA heteroplasmy levels when mitochondrial division is defective.

Based on our results only mtDNA segregation in the hematopoietic compartment appears to be modulated by a defect in mitochondrial division. Previously we identified two paralogues, *Gimap3* and *Gimap5*, of the vertebrate conserved *Gimap* (GTPase immunity associated protein) gene cluster on mouse chromosome 6 as modifiers of mtDNA selection in the hematopoietic compartment (44,45). Gimaps are GTPases structurally related to septins and dynamins and proposed to form scaffolds (52,53). A tail anchor sequence in Gimap3 localizes the protein to the ER (45), whereas Gimap5 is lysosomal (54). Quantitative differences in the abundance of Gimap3 and Gimap5 modify the selection of mtDNA in leukocytes (45).

It is worth noting that the effect of Gimaps on mtDNA segregation were also independent of mtDNA copy number (44). Together, these findings suggest that in leukocytes mitochondrial morphology and interactions with other organelles appear to be important factors to segregation of the mitochondrial genome.

In conclusion, our study demonstrates genetically a robust organization of a heteroplasmic mtDNA segregating unit that appears to overcome defects in mitochondrial division. Future work is required to generate greater resolution at the cytological level for the organization of heteroplasmic nucleoids and what defines the segregating unit physically across cell types differing in mtDNA copy number and membrane morphology.

Materials and Methods

Mouse experiments and ethical statement

All mouse experiments were approved by the National Animal Experiment Board of Finland and maintained in a barrier facility

at the Laboratory Animal Centre of the University of Helsinki. On the nuclear background of *Mus musculus domesticus* strains there are no differences on the segregation of the BALB and NZB mtDNA haplotypes across tissues (42,43) or in the germline transmission (3). The mouse crosses were as follows: female heteroplasmic mice (BALB/c background) were outcrossed to males *Dnm1l*$^{+/Py}$ (C57BL/6 background); F1 females *Dnm1l*$^{+/Py}$ (C57BL/6 X BALB/c) were backcrossed to BALB/c males and the N2 progeny analyzed for mtDNA transmission through the female germline and for assessing mtDNA segregation post-natally in tissues. Mice were housed in random groups and sampled for tissue collection in random order at 90 ± 2 days of age.

mtDNA analysis

Total DNA was extracted with phenol-chloroform and mtDNA heteroplasmy level determined as described previously (37). mtDNA copy number was determined by qPCR, where the relative level of mtDNA to nuclear DNA was determined using iQ SYBR Green (Bio-Rad) on a Bio-Rad CFX96 C1000 Touch Thermal Cycler with primers for mtDNA and the single-copy nuclear gene β-2 microglobulin (44). All samples were run in triplicate.

Cell culture

Mouse embryonic fibroblasts (MEFs) were isolated from *Dnm1l*$^{+/+}$ and *Dnm1l*$^{+/Py}$ embryos and cultured in Dulbecco's modified Eagle's medium (Lonza) with high glucose supplemented with 10% fetal bovine serum, 1× glutamax and 50 mg/ml uridine. The K38E Dnm1l cDNA (kind gift of Heidi McBride) was transiently transfected with JetPrime (Polypus Transfection).

Microscopy

MEFs were grown on coverslips and washed several times in phosphate buffered saline (PBS), fixed in 4% paraformaldehyde for 15 min, washed in PBS, then treated with 100% methanol for 5 min and washed again in PBS. Cells were blocked in 5% bovine serum albumin /PBST (PBS + 0.1% Tween 20) then incubated with mouse anti-Sdha (C2061 MitoSciences/Abcam) 1:250 for 1 h at room temperature. Cells were washed several times in PBST before incubation with anti-mouse Alexa 594 1:1000 (Life Technologies) for 1 h. Before mounting cells were washed several times in PBST. Cells were mounted with DABCO/MOWIOL on glass slides for confocal imaging with a Leica TCS CARS SP8 motorized DMI 6000 inverted microscope at room temperature using a 63× HC PL APO CS2 (1.2 NA) water objective with DPSS (561 nm) laser. Images were acquired with a Hybrid GaAsP detector with the Leica LAS AF software and then exported into Image J using the Fiji plug-in to apply brightness and contrast adjustments.

Statistical analysis

Animals with an initial heteroplasmy of 20–80% NZB mtDNA from the ear punch were included in the analysis assessing mtDNA segregation in tissues. Non-linear regression analysis was performed with GraphPad Prism 6.0. Data was tested for normality (D'agostino & Pearson and Shapiro-Wilk tests) before proceeding with parametric statistical analysis (two-tailed *t*-test). The relative fitness for the NZB mtDNA haplotype in the liver was calculated as described in Ref. (37). In the spleen there is selection against the NZB mtDNA haplotype so the proportion of NZB mtDNA remaining in the tissue is calculated (43).

The relative proportion of NZB mitochondria in mother-offspring sets was compared with the neutral hypothesis estimated by the Kimura distribution. We used the Kimura003.c software (46). The mother's relative proportion NZB (*p*), the number of offspring (*N*) and the variance in the relative levels of the offspring (*var*) were hand edited for each data set as directed in the accompanying readme file. In the analysis offspring were grouped at 1% intervals for their relative levels of the NZB haplotype. Due to the limited number of offspring per female, in some cases we grouped females of similar relative levels for analysis to increase the statistical power of our analysis. In the combined data sets, the weighted mean of the females' proportion of NZB as the *p* variable. The *P*-values were obtained *P*-values determined from Monte-Carlo simulations (46). Graphs were generated in Graphpad Prism 6.0 from the output data.

Blood analysis

Total blood samples were collected by cardiac puncture to ethylenediaminetetraacetic acid coated tubes immediately after euthanasia. Samples were analyzed the same day at the University of Helsinki Small Animal Hospital with an Advia 2120i analyzer.

Supplementary Material

Supplementary Material is available at *HMG* online.

Acknowledgements

We thank Uwe Richter for discussion and the Biomedicum Imaging Unit for the confocal facilities.

Conflict of Interest statement. None declared.

Funding

This work was supported by funding to B.J.B. from the Jane and Aatos Erkko Foundation, the Academy of Finland and University of Helsinki. R.J. was funded by the Doctoral Programme in Biomedicine of the Doctoral School in Health Sciences (University of Helsinki), the Finnish Cultural Foundation, the Biomedicum-Helsinki Foundation, Emil Aaltonen's Foundation and Waldemar von Frenckell's Foundation. T.N.D. was supported by a project grant from the British Heart Foundation.

References

1. Hauswirth, W.W. and Laipis, P.J. (1982) Mitochondrial DNA polymorphism in a maternal lineage of Holstein cows. *Proc. Natl Acad. Sci. USA*, **79**, 4686–4690.
2. Olivo, P.D., Van de Walle, M.J., Laipis, P.J. and Hauswirth, W.W. (1983) Nucleotide sequence evidence for rapid genotypic shifts in the bovine mitochondrial DNA D-loop. *Nature*, **306**, 400–402.
3. Jenuth, J.P., Peterson, A.C., Fu, K. and Shoubridge, E.A. (1996) Random genetic drift in the female germline explains the rapid segregation of mammalian mitochondrial DNA. *Nat. Genet.*, **14**, 146–151.
4. Cree, L.M., Samuels, D.C., de Sousa Lopes, S.C., Rajasimha, H. K., Wonnapinij, P., Mann, J.R., Dahl, H.H. and Chinnery, P.F. (2008) A reduction of mitochondrial DNA molecules during embryogenesis explains the rapid segregation of genotypes. *Nat. Genet.*, **40**, 249–254.

5. Wai, T., Teoli, D. and Shoubridge, E.A. (2008) The mitochondrial DNA genetic bottleneck results from replication of a subpopulation of genomes. *Nat. Genet.*, **40**, 1484–1488.
6. Stewart, J.B., Freyer, C., Elson, J.L., Wredenberg, A., Cansu, Z., Trifunovic, A. and Larsson, N.G. (2008) Strong purifying selection in transmission of mammalian mitochondrial DNA. *PLoS Biol.*, **6**, e10.
7. Samuels, D.C., Wonnapinij, P., Cree, L.M. and Chinnery, P.F. (2010) Reassessing evidence for a postnatal mitochondrial genetic bottleneck. *Nat. Genet.*, **42**, 471–472; author reply 472–473.
8. Kaufman, B.A., Durisic, N., Mativetsky, J.M., Costantino, S., Hancock, M.A., Grutter, P. and Shoubridge, E.A. (2007) The mitochondrial transcription factor TFAM coordinates the assembly of multiple DNA molecules into nucleoid-like structures. *Mol. Biol. Cell*, **18**, 3225–3236.
9. Kukat, C., Wurm, C.A., Spahr, H., Falkenberg, M., Larsson, N.G. and Jakobs, S. (2011) Super-resolution microscopy reveals that mammalian mitochondrial nucleoids have a uniform size and frequently contain a single copy of mtDNA. *Proc. Natl Acad. Sci. USA*, **108**, 13534–13539.
10. Brown, T.A., Tkachuk, A.N., Shtengel, G., Kopek, B.G., Bogenhagen, D.F., Hess, H.F. and Clayton, D.A. (2011) Superresolution fluorescence imaging of mitochondrial nucleoids reveals their spatial range, limits, and membrane interaction. *Mol. Cell. Biol.*, **31**, 4994–5010.
11. Bogenhagen, D.F., Wang, Y., Shen, E.L. and Kobayashi, R. (2003) Protein components of mitochondrial DNA nucleoids in higher eukaryotes. *Mol. Cell. Proteomics*, **2**, 1205–1216.
12. Hensen, F., Cansiz, S., Gerhold, J.M. and Spelbrink, J.N. (2014) To be or not to be a nucleoid protein: a comparison of mass-spectrometry based approaches in the identification of potential mtDNA-nucleoid associated proteins. *Biochimie*, **100**, 219–226.
13. Mishra, P. and Chan, D.C. (2014) Mitochondrial dynamics and inheritance during cell division, development and disease. *Nat. Rev. Mol. Cell Biol.*, **15**, 634–646.
14. Chen, H., Vermulst, M., Wang, Y.E., Chomyn, A., Prolla, T.A., McCaffery, J.M. and Chan, D.C. (2010) Mitochondrial fusion is required for mtDNA stability in skeletal muscle and tolerance of mtDNA mutations. *Cell*, **141**, 280–289.
15. Labbe, K., Murley, A. and Nunnari, J. (2014) Determinants and functions of mitochondrial behavior. *Annu. Rev. Cell Dev. Biol.*, **30**, 357–391.
16. Garrido, N., Griparic, L., Jokitalo, E., Wartiovaara, J., van der Bliek, A.M. and Spelbrink, J.N. (2003) Composition and dynamics of human mitochondrial nucleoids. *Mol. Biol. Cell*, **14**, 1583–1596.
17. Legros, F., Malka, F., Frachon, P., Lombes, A. and Rojo, M. (2004) Organization and dynamics of human mitochondrial DNA. *J. Cell Sci.*, **117**, 2653–2662.
18. Murley, A., Lackner, L.L., Osman, C., West, M., Voeltz, G.K., Walter, P. and Nunnari, J. (2013) ER-associated mitochondrial division links the distribution of mitochondria and mitochondrial DNA in yeast. *eLife*, **2**, e00422.
19. Ford, M.G., Jenni, S. and Nunnari, J. (2011) The crystal structure of dynamin. *Nature*, **477**, 561–566.
20. Frohlich, C., Grabiger, S., Schwefel, D., Faelber, K., Rosenbaum, E., Mears, J., Rocks, O. and Daumke, O. (2013) Structural insights into oligomerization and mitochondrial remodelling of dynamin 1-like protein. *EMBO J.*, **32**, 1280–1292.
21. Mears, J.A., Lackner, L.L., Fang, S., Ingerman, E., Nunnari, J. and Hinshaw, J.E. (2011) Conformational changes in Dnm1 support a contractile mechanism for mitochondrial fission. *Nat. Struct. Mol. Biol.*, **18**, 20–26.
22. Ishihara, T., Ban-Ishihara, R., Maeda, M., Matsunaga, Y., Ichimura, A., Kyogoku, S., Aoki, H., Katada, S., Nakada, K., Nomura, M. *et al.* (2015) Dynamics of mitochondrial DNA nucleoids regulated by mitochondrial fission is essential for maintenance of homogeneously active mitochondria during neonatal heart development. *Mol. Cell. Biol.*, **35**, 211–223.
23. Rohn, J.L., Patel, J.V., Neumann, B., Bulkescher, J., McHedlishvili, N., McMullan, R.C., Quintero, O.A., Ellenberg, J. and Baum, B. (2014) Myo19 ensures symmetric partitioning of mitochondria and coupling of mitochondrial segregation to cell division. *Curr. Biol.*, **24**, 2598–2605.
24. Wakabayashi, J., Zhang, Z., Wakabayashi, N., Tamura, Y., Fukaya, M., Kensler, T.W., Iijima, M. and Sesaki, H. (2009) The dynamin-related GTPase Drp1 is required for embryonic and brain development in mice. *J. Cell Biol.*, **186**, 805–816.
25. Ishihara, N., Nomura, M., Jofuku, A., Kato, H., Suzuki, S.O., Masuda, K., Otera, H., Nakanishi, Y., Nonaka, I., Goto, Y. *et al.* (2009) Mitochondrial fission factor Drp1 is essential for embryonic development and synapse formation in mice. *Nat. Cell Biol.*, **11**, 958–966.
26. Udagawa, O., Ishihara, T., Maeda, M., Matsunaga, Y., Tsukamoto, S., Kawano, N., Miyado, K., Shitara, H., Yokota, S., Nomura, M. *et al.* (2014) Mitochondrial fission factor Drp1 maintains oocyte quality via dynamic rearrangement of multiple organelles. *Curr. Biol.*, **24**, 2451–2458.
27. Waterham, H.R., Koster, J., van Roermund, C.W., Mooyer, P.A., Wanders, R.J. and Leonard, J.V. (2007) A lethal defect of mitochondrial and peroxisomal fission. *N. Engl. J. Med.*, **356**, 1736–1741.
28. Ashrafian, H., Docherty, L., Leo, V., Towlson, C., Neilan, M., Steeples, V., Lygate, C.A., Hough, T., Townsend, S., Williams, D. *et al.* (2010) A mutation in the mitochondrial fission gene Dnm1l leads to cardiomyopathy. *PLoS Genet.*, **6**, e1001000.
29. Stewart, J.B. and Larsson, N.G. (2014) Keeping mtDNA in shape between generations. *PLoS Genet.*, **10**, e1004670.
30. Wai, T., Ao, A., Zhang, X., Cyr, D., Dufort, D. and Shoubridge, E.A. (2010) The role of mitochondrial DNA copy number in mammalian fertility. *Biol. Reprod.*, **83**, 52–62.
31. Piko, L. and Chase, D.G. (1973) Role of the mitochondrial genome during early development in mice. Effects of ethidium bromide and chloramphenicol. *J. Cell Biol.*, **58**, 357–378.
32. Wakai, T., Harada, Y., Miyado, K. and Kono, T. (2014) Mitochondrial dynamics controlled by mitofusins define organelle positioning and movement during mouse oocyte maturation. *Mol. Hum. Reprod.*, **20**, 1090–1100.
33. Motta, P.M., Nottola, S.A., Makabe, S. and Heyn, R. (2000) Mitochondrial morphology in human fetal and adult female germ cells. *Hum. Reprod.*, **15**(Suppl. 2), 129–147.
34. Sathananthan, A.H. and Trounson, A.O. (2000) Mitochondrial morphology during preimplantational human embryogenesis. *Hum. Reprod.*, **15**(Suppl. 2), 148–159.
35. Malena, A., Loro, E., Di Re, M., Holt, I.J. and Vergani, L. (2009) Inhibition of mitochondrial fission favours mutant over wild-type mitochondrial DNA. *Hum. Mol. Genet.*, **18**, 3407–3416.
36. Jokinen, R. and Battersby, B.J. (2013) Insight into mammalian mitochondrial DNA segregation. *Ann. Med.*, **45**, 149–155.
37. Battersby, B.J. and Shoubridge, E.A. (2001) Selection of a mtDNA sequence variant in hepatocytes of heteroplasmic mice is not due to differences in respiratory chain function or efficiency of replication. *Hum. Mol. Genet.*, **10**, 2469–2479.
38. Moreno-Loshuertos, R., Acin-Perez, R., Fernandez-Silva, P., Movilla, N., Perez-Martos, A., Rodriguez de Cordoba, S.,

Gallardo, M.E. and Enriquez, J.A. (2006) Differences in reactive oxygen species production explain the phenotypes associated with common mouse mitochondrial DNA variants. *Nat. Genet.*, **38**, 1261–1268.
39. Chinnery, P.F., Thorburn, D.R., Samuels, D.C., White, S.L., Dahl, H.M., Turnbull, D.M., Lightowlers, R.N. and Howell, N. (2000) The inheritance of mitochondrial DNA heteroplasmy: random drift, selection or both? *Trends Genet.*, **16**, 500–505.
40. Freyer, C., Cree, L.M., Mourier, A., Stewart, J.B., Koolmeister, C., Milenkovic, D., Wai, T., Floros, V.I., Hagstrom, E., Chatzidaki, E.E. *et al.* (2012) Variation in germline mtDNA heteroplasmy is determined prenatally but modified during subsequent transmission. *Nat. Genet.*, **44**, 1282–1285.
41. Jenuth, J.P., Peterson, A.C. and Shoubridge, E.A. (1997) Tissue-specific selection for different mtDNA genotypes in heteroplasmic mice. *Nat. Genet.*, **16**, 93–95.
42. Battersby, B.J., Loredo-Osti, J.C. and Shoubridge, E.A. (2003) Nuclear genetic control of mitochondrial DNA segregation. *Nat. Genet.*, **33**, 183–186.
43. Battersby, B.J., Redpath, M.E. and Shoubridge, E.A. (2005) Mitochondrial DNA segregation in hematopoietic lineages does not depend on MHC presentation of mitochondrially encoded peptides. *Hum. Mol. Genet.*, **14**, 2587–2594.
44. Jokinen, R., Marttinen, P., Sandell, H.K., Manninen, T., Teerenhovi, H., Wai, T., Teoli, D., Loredo-Osti, J.C., Shoubridge, E.A. and Battersby, B.J. (2010) Gimap3 regulates tissue-specific mitochondrial DNA segregation. *PLoS Genet.*, **6**, e1001161.
45. Jokinen, R., Lahtinen, T., Marttinen, P., Myohanen, M., Ruotsalainen, P., Yeung, N., Shvetsova, A., Kastaniotis, A.J., Hiltunen, J.K., Ohman, T. *et al.* (2015) Quantitative changes in Gimap3 and Gimap5 expression modify mitochondrial DNA segregation in mice. *Genetics*, **200**, 221–235.
46. Wonnapinij, P., Chinnery, P.F. and Samuels, D.C. (2008) The distribution of mitochondrial DNA heteroplasmy due to random genetic drift. *Am. J. Hum. Genet.*, **83**, 582–593.
47. Rajasimha, H.K., Chinnery, P.F. and Samuels, D.C. (2008) Selection against pathogenic mtDNA mutations in a stem cell population leads to the loss of the 3243A–>G mutation in blood. *Am. J. Hum. Genet.*, **82**, 333–343.
48. Friedman, J.R., Lackner, L.L., West, M., DiBenedetto, J.R., Nunnari, J. and Voeltz, G.K. (2011) ER tubules mark sites of mitochondrial division. *Science*, **334**, 358–362.
49. Kornmann, B., Currie, E., Collins, S.R., Schuldiner, M., Nunnari, J., Weissman, J.S. and Walter, P. (2009) An ER-mitochondria tethering complex revealed by a synthetic biology screen. *Science*, **325**, 477–481.
50. Chinnery, P.F. and Samuels, D.C. (1999) Relaxed replication of mtDNA: a model with implications for the expression of disease. *Am. J. Hum. Genet.*, **64**, 1158–1165.
51. Wasserstrom, A., Frumkin, D., Adar, R., Itzkovitz, S., Stern, T., Kaplan, S., Shefer, G., Shur, I., Zangi, L., Reizel, Y. *et al.* (2008) Estimating cell depth from somatic mutations. *PLoS Comput. Biol.*, **4**, e1000058.
52. Schwefel, D., Frohlich, C., Eichhorst, J., Wiesner, B., Behlke, J., Aravind, L. and Daumke, O. (2010) Structural basis of oligomerization in septin-like GTPase of immunity-associated protein 2 (GIMAP2). *Proc. Natl Acad. Sci. USA*, **107**, 20299–20304.
53. Schwefel, D., Arasu, B.S., Marino, S.F., Lamprecht, B., Kochert, K., Rosenbaum, E., Eichhorst, J., Wiesner, B., Behlke, J., Rocks, O. *et al.* (2013) Structural insights into the mechanism of GTPase activation in the GIMAP family. *Structure*, **21**, 550–559.
54. Wong VWY, S.A., Hutchings, A., Pascall, J.C., Carter, C., Bright, N., Walker, S.A., Ktistakis, N.T. and Butcher, G.W. (2010) The autoimmunity-related GIMAP5 GTPase is a lysosome-associated protein. *Self Nonself*, **1**, 259–268.